High-pressure-induced spin-liquid phase of multiferroic $YMnO_3$

D. P. Kozlenko,[1] I. Mirebeau,[2] J.-G. Park,[3,4] I. N. Goncharenko,[2] S. Lee,[3] Junghwan Park,[3] and B. N. Savenko[1]
[1]*Frank Laboratory of Neutron Physics, Joint Institute for Nuclear Research, 141980 Dubna, Russia*
[2]*Laboratoire Léon Brillouin, CEA-CNRS, CE Saclay, 91191 Gif-sur-Yvette, France*
[3]*Department of Physics, SungKyunKwan University, Suwon 440-746, Republic of Korea*
[4]*Center for Strongly Correlated Materials Research, Seoul National University, Seoul 151-742, Republic of Korea*
(Received 25 June 2008; published 1 August 2008)

We investigated the magnetic structure and short-range spin correlations of multiferroic hexagonal manganite $YMnO_3$ by powder neutron diffraction at high pressures up to 6.7 GPa. High pressure induces a spin-liquid phase in multiferroic $YMnO_3$, coexisting with the suppressed long-range antiferromagnetic order. This spin-liquid phase exhibits a temperature dependence distinctively different from short-range spin correlations seen at ambient pressure. Its formation occurs through an in-plane Mn-O bond symmetrization and results in reduced magnetoelastic coupling at high pressures.

DOI: 10.1103/PhysRevB.78.054401 PACS number(s): 75.25.+z, 75.50.Ee, 61.50.Ks

I. INTRODUCTION

Materials that show the coexistence of ferroelectric and magnetic phases are unusual but not totally rare. For a long time, the so-called multiferroic materials have remained a mystery as well as a huge challenge to material science communities.[1] However, recent extensive investigations have been continuously bringing a list of materials with such a phenomenon.[2] This rediscovery has already shown quite interesting physics such as switching electric polarization by magnetic field and a possible composite excitation of electromagnon, and promises many more surprises awaiting to be unearthed.[3] Despite this, coupling mechanisms between magnetic ordering and ferroelectricity and their nature remain unclear and are under extensive studies at the moment.

The hexagonal manganites $R\mathrm{MnO}_3$ (R=Ho, Er, Tm, Yb, Lu, Y, Sc, and In) are a unique class of materials, exhibiting multiferroic phenomenon in combination with frustrated low dimensional magnetism on triangular lattice.[2–8] In these compounds, the ferroelectric transition temperature $T_C \sim 600-900$ K is much higher in comparison with the antiferromagnetic (AFM) ordering temperature, $T_N \sim 70-130$ K.[6] However, we note that magnetic Curie-Weiss temperatures are in the range of 500–700 K for most of hexagonal $R\mathrm{MnO}_3$, more than seven times that of T_N, which indicates that the Mn moments are strongly frustrated.[9,10]

In the hexagonal $R\mathrm{MnO}_3$ structure of $P6_3cm$ symmetry, Mn ions are located at the centers of MnO_5 bipyramids and they form a natural two-dimensional edge-sharing triangular network separated along the c axis by a noncoplanar layer of R atoms. The distance between the nearest Mn atoms is $\sim$3.5 Å in the ab plane and $\sim$6 Å along the c axis, respectively. This then leads naturally to geometrically frustrated magnetism with strong in-plane Mn-O-Mn antiferromagnetic superexchange interactions while the Mn-O-O-Mn superexchange between adjacent triangular planes is about two orders of magnitude weaker.[11,12]

The hexagonal manganites form an important class of model magnetic systems with a delicate balance between the competing long-range AFM and the short-range spin-liquid states on the triangular lattice. For instance, $YMnO_3$ exhibits a triangular AFM structure of Γ_1 (or Γ_3) irreducible representation symmetry below T_N=75 K and, simultaneously, strong spin fluctuations above T_N.[5,11,13–15] These spin fluctuations are understood to arise from the formation of an intermediate spin-liquid state.[14]

Recent high-pressure studies found that the ordered Mn magnetic moments of $YMnO_3$ and $LuMnO_3$ are strongly suppressed at low temperatures, implying significantly enhanced spin fluctuations in both compounds at high pressures.[16–18] However, latest muon spin-relaxation (μSR) experiments observed T_N of $YMnO_3$ to increase with pressures up to 1.4 GPa while no evidence of the spin-liquid state was found below T_N.[19] These somewhat contrasting observations clearly show that the nature of the magnetic state of $YMnO_3$ at high pressures, especially the relationship between the pressure-enhanced T_N and the spin fluctuations, still remains unanswered. Our high-pressure neutron-diffraction experiments reveal how exactly the missing spin-liquid phase evolves with pressure. Furthermore, our analysis shows that the high-pressure-induced spin-liquid phase occurs through increased frustration due to an in-plane Mn-O bond symmetrization.

II. EXPERIMENT DETAILS

Polycrystalline $YMnO_3$ sample was synthesized by using the standard solid-state reaction method.[14] X-ray diffraction measurements at room temperature showed that our sample forms in the single phase of the hexagonal $P6_3cm$ structure. Neutron powder-diffraction measurements were performed with the G6.1 diffractometer using a setup for high-pressure experiments[20] at the Orphée reactor (Laboratoire Leon Brillouin). An incident neutron wavelength was 4.74 Å. Sample with a volume of $\sim$1 mm^3 was loaded into a sapphire anvil high-pressure cell.[21] As a pressure transmitting medium, NaCl was admixed to the sample in a 1:2 volume ratio and pressure was measured by the ruby fluorescence technique. All our experiments were carried out in the pressure range of 0–6.7 GPa and the temperature range of 1.5–300 K. In order to study the crystal structure of $YMnO_3$, additional high-pressure experiments were performed with the DN-12 spec-

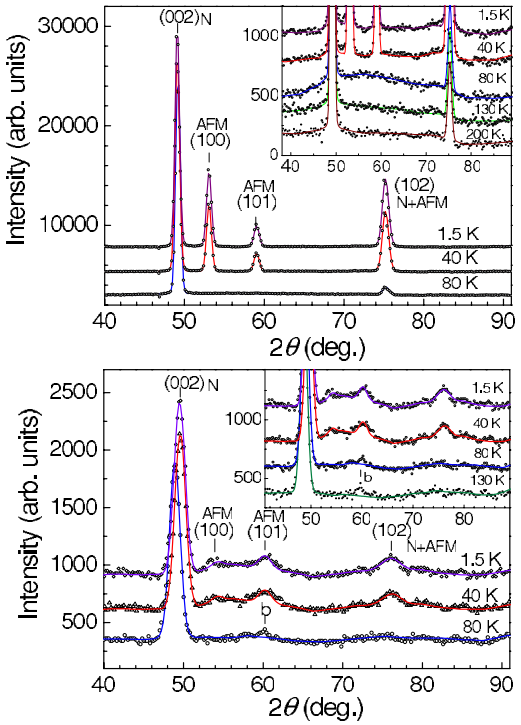

FIG. 1. (Color online) Neutron-diffraction patterns of $YMnO_3$ measured at ambient pressure (top) and 6.7 GPa (bottom) at selected temperatures. Symbols and solid lines represent experimental points and Rietveld refinement results. The insets are enlarged pictures of the diffuse scattering for the same data. The indexes of nuclear and magnetic Bragg peaks are also given. A spurious peak from pressure cell is marked by "b" in the bottom figure.

trometer at the IBR-2 pulsed reactor (Frank Laboratory of Neutron Physics, Joint Institute for Nuclear Research) using sapphire pressure cell. The diffraction data were analyzed by the Rietveld method using the FULLPROF and MRIA programs.[22,23]

III. RESULTS AND DISCUSSION

Neutron-diffraction patterns of $YMnO_3$ measured at the G6.1 diffractometer at different pressures and temperatures are shown in Fig. 1. At ambient pressure a broad diffuse scattering appears at $40<2\theta<80°$ for temperatures well above $T_N=75$ K. Upon cooling the diffuse scattering gets stronger and reaches a maximum at T_N (Fig. 1). Using a Selyakov-Scherrer formula $\xi\approx\lambda/\Delta(2\theta)\cos\theta$, we have estimated the correlation length of $\xi\approx 11$ Å characterizing spin fluctuations, in good agreement with previous estimates for ambient pressure.[14] Below T_N, however, the magnetic diffuse scattering is rapidly suppressed, and, at the same time, new magnetic peaks (100) and (101) appear at $d=5.31$ and 4.82 Å, respectively, indicating an onset of the triangular 120° AFM state of Γ_1 symmetry.[5,12–14] The value of the ordered Mn magnetic moment is determined to be $3.20(5)\mu_B$ at $T=1.5$ K, similar to the previous studies of $YMnO_3$ at ambient pressure.[5,11,13,14] We note that the ordered moment is considerably smaller than the full ionic value of $4.0\mu_B$ for Mn^{3+}, which was then interpreted as another piece of experimental evidence in support of strong spin fluctuations at low temperatures.[14]

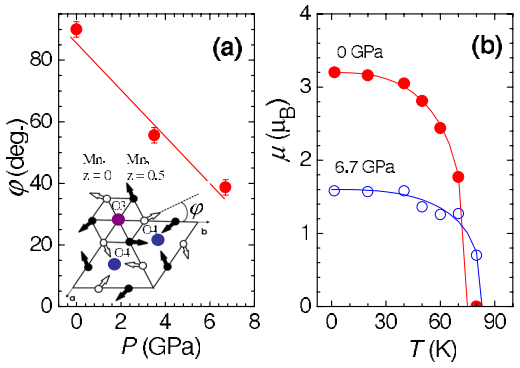

FIG. 2. (Color online) (a) The pressure dependence of the angle φ between Mn magnetic moments (at 10 K) and hexagonal axes in $YMnO_3$. The line is a guide to eyes. The inset in (a) shows how the magnetic structure changes from initial Γ_1 ($\varphi=90°$) toward $\Gamma_1+\Gamma_2$ ($0°<\varphi<90°$). (b) The temperature dependences of the ordered Mn magnetic moments for $YMnO_3$ at $P=0$ and 6.7 GPa.

At high pressure of $P=6.7$ GPa, we observed a substantial decrease and, more importantly, a visible relative change in the intensities of the magnetic peaks at low temperatures, compared with the ambient pressure data (Fig. 1). Our subsequent analysis using Rietveld refinement duly found that at 6.7 GPa the ordered Mn magnetic moments get further reduced from $3.2\mu_B$ to $1.6\mu_B$ and, simultaneously, undergo a pressured-induced reorientation in the *ab* plane, as reported in the previous studies for a smaller pressure range.[16,18] The angle φ between the Mn magnetic moments and the hexagonal $\boldsymbol{a}$, $\boldsymbol{b}$, and $\boldsymbol{u}=-(\boldsymbol{a}+\boldsymbol{b})$ axes decreases continuously from 90° to 38° with increasing external pressure from 0 to 6.7 GPa [Fig. 2(a)]. It implies that the symmetry of the triangular AFM state of $YMnO_3$ changes from a pure Γ_1 ($\varphi=90°$) to a mixed $\Gamma_1+\Gamma_2$ irreducible representation [Fig. 2(a)]. During our refinements of the data using the latter model, the angle φ value was allowed to vary freely between 90° and 0° as a fitting parameter.

From the measured temperature dependence of the ordered Mn magnetic moment [Fig. 2(b)], we obtained $T_N=83$ K at $P=6.7$ GPa. If we assume a linear pressure dependence of T_N, it corresponds roughly to the average pressure coefficient of $dT_N/dP=1.2$ K/GPa, somewhat smaller than the value of 3 K/GPa that was estimated from the muon spin relxation data taken at a moderate pressure range up to 1.4 GPa.[19]

Of particular notice is that, at high pressures, the temperature evolution of the diffuse scattering is drastically modified (Figs. 1 and 3). For example, it is almost negligible above T_N at $P=6.7$ GPa whereas it becomes stronger and reaching a maximum near T_N at ambient pressure [Fig. 3(a)]. However, under high pressure it increases gradually on cooling below T_N and reaches a maximum intensity at the lowest measured temperature of our study, $T=1.5$ K. At the same time the diffuse scattering peak becomes much narrower with pressure [see Fig. 3(c)]. The corresponding correlation length estimated from the Selyakov-Scherrer formula increases to $\xi\approx 22$ Å, twice the value estimated at ambient pressure and $T\sim T_N$.

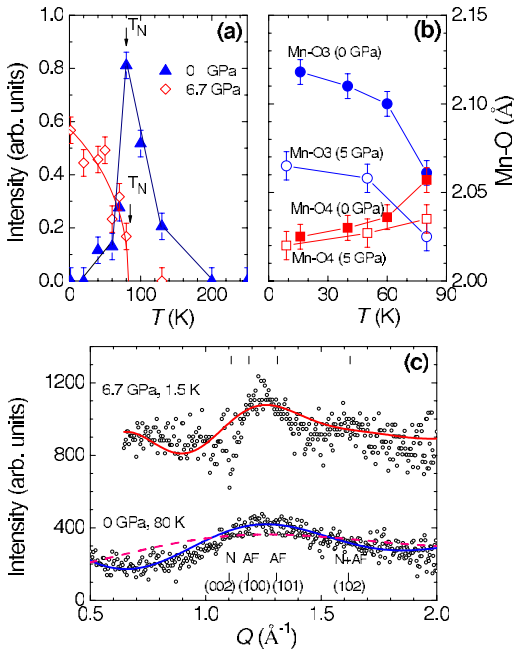

FIG. 3. (Color online) (a) Temperature dependences of the integrated intensity of diffuse scattering peak in $YMnO_3$ at $P=0$ and 6.7 GPa, normalized by the intensity of nuclear peak (002), which is weakly dependent on pressure. The integration was performed over the Q range of 0.7–1.9 Å^{-1}. (b) Temperature dependences of Mn-O3 and Mn-O4 bond distances below and in vicinity of T_N in $YMnO_3$ at $P=0$ and 5 GPa. (c) Characteristic difference patterns of $YMnO_3$ at $P=0$ GPa and $T=80$ K (obtained by subtracting the data measured at $T=250$ K), and $P=6.7$ GPa and $T=1.5$ K (obtained by subtracting the data measured at $T=130$ K and the calculated magnetic long-range AFM contribution), representing the magnetic diffuse scattering. Solid lines represent fitting results of the diffraction data using a function $I(Q)$ with two (six) terms for the ambient (high) pressure, as described in the text. Dashed line corresponds to fitting results of ambient pressure data using correlations between the nearest-neighbor spins only. Indexes of nuclear (N) and magnetic (AF) Bragg peaks are also given.

In order to further clarify the nature of the short-range spin correlations in $YMnO_3$, we obtained the characteristic magnetic diffuse scattering data [Fig. 3(c)] by subtracting off the nuclear contributions ($P=0$ and 6.7 GPa, and $T=80$ and 1.5 K) and contributions from the AFM long-range order ($P=6.7$ GPa and $T=1.5$ K). For the analysis we then used the following formula:[24]

$$\frac{I(Q)}{F^2(Q)} \sim \sum_{i,j} \langle \vec{S}_i \vec{S}_j \rangle \frac{\sin Q r_{ij}}{r_{ij}},$$

where $I(Q)$ is the measured intensity of diffuse scattering, $F(Q)$ the magnetic form factor[25] of Mn^{3+} ion, $Q=4\pi \sin\theta/\lambda$ the momentum transfer, and r_{ij} the distance between neighboring spins $\vec{S}_i$ and $\vec{S}_j$. We note that this formula was successfully applied to describe diffuse scatterings in various magnetic materials such as short-range ordered magnets, spin glasses, and other frustrated magnetic systems.[24,26,27]

As we can see in Fig. 3(c), the magnetic diffuse scattering that was observed at ambient pressure and $T=80$ K $\sim T_N$ can be well described by taking into account both nearest neighboring spins at $r_{ij} \approx 3.54$ Å, and next-nearest-neighboring spins at $r_{ij}=6.13$ Å, as in the previous study.[14] One should note that the $2\times r_{ij}$ value with $r_{ij}=6.13$ Å is very close to the correlation length $\xi \approx 11$ Å estimated from the Selyakov-Scherrer formula aforementioned. If only nearest neighboring spins are considered, the fitting quality becomes apparently worse [dashed line in Fig. 3(c)]. We also note that the prefactor of $\langle \vec{S}_i \vec{S}_j \rangle$ in the formula has a negative sign for the nearest neighboring spins while it has a positive sign for the next-nearest-neighboring spins with the ratio of −0.4, in agreement with the ideal value of −0.5 for the long-range 120° AFM structure.

As we commented above, the correlation length ξ of the diffuse scattering increases with pressures. This implies strongly that one needs to take into account correlations between spins much farther apart in order to explain the experimental observations at high pressure than those done for the ambient pressure data. In fact, we found from the fitting of the diffuse scattering data obtained at $P=6.7$ GPa and $T=1.5$ K that it is necessary for us to consider at least six coordination shells with interatomic distances between spins up to $r_{ij}=12.1$ Å to describe the diffuse scattering satisfactorily. We note that the $2\times r_{ij}$ value with $r_{ij}=12.1$ Å is very close to the correlation length $\xi \approx 22$ Å estimated from the Selyakov-Scherrer formula. However, due to strong correlations between different $\langle \vec{S}_i \vec{S}_j \rangle$ coefficients, it was difficult to estimate all their values reliably. As we discussed for the ambient pressure data, the short-range magnetic order appears to share similar features of the long-range AFM order. In first approximation it is also reasonable for us to assume that the symmetry of the short-range magnetic order at high pressures remains also similar to the long-range AFM one. Under this assumption, we obtained a satisfactory description of the experimental data [Fig. 3(c)] using values $\langle \vec{S}_i \vec{S}_j \rangle = 1$ for $i=j$ and $i=3n+m$, $j=m$ ($n=1,2,\ldots; m=0,1,2,\ldots$), and $\langle \vec{S}_i \vec{S}_j \rangle = -1/2$ for all the other pairs of (i,j), which correspond exactly to the ideal case of the AFM 120° long-range order.

In marked contrast to the ambient pressure data, our high-pressure data show that both magnetic peaks of the long-range AFM order and the diffuse scattering due to spin fluctuations exhibit similar temperature dependence to one another below T_N: their intensity grows stronger as it cools to lower temperatures. All this happens at the same time when the ordered magnetic moment is significantly reduced from its ambient pressure value. This then implies that the ground state at high pressures is antiferromagnetic with strong short-range spin fluctuations. The striking difference in the temperature dependence of the diffuse scattering between ambient pressure and 6.7 GPa [Fig. 3(a)] is a very strong piece of evidence supporting the idea of the coexistence of the suppressed long-range order and the pressure-induced spin-liquid ground state in $YMnO_3$ at high pressures. We should note that the presence of a spin-liquid ground state was not identified for $YMnO_3$ in the latest μSR experiments[19] at moderate pressures up to 1.4 GPa, implying its stabilization

for higher pressure range only. At the same time, T_N gets increased with pressure at a rate of $dT_N/dP=1.2$ K/GPa.

How can we understand these experimental observations? In the hexagonal crystal structure of $YMnO_3$, there are two types of in-plane bonds:[28] Mn-O3 and Mn-O4 [see the inset of Fig. 2(a)], whose values control the delicate balance of the dominant Mn-O3-Mn and Mn-O4-Mn superexchange AFM interactions within the Mn triangular network. In order to study the pressure dependence and, in particular, the temperature dependences of the in-plane Mn-O bonds, we measured neutron-diffraction data for $T<80$ K and $P=0$ and 5 GPa with the DN-12 spectrometer. Interestingly enough, we observed in these new data that the Mn-O3 and Mn-O4 bonds became very close to one another at ambient pressure and $T=80$ K, where the diffuse scattering reaches a maximum, with the difference being just about 0.005 Å above T_N [Fig. 3(b)]. As one can see in the figure, upon cooling below T_N, the onset of the AFM triangular state is accompanied by a noticeable splitting of these two bonds. The difference between their lengths reaches a value of 0.09 Å at $T=10$ K. This splitting in the Mn-O bonds then lifts up the geometrical frustration effects in the ordered phase at ambient pressure. Moreover, such a drastic splitting in the in-plane Mn-O bond distances at ambient pressure has been recently interpreted as evidence of large magnetoelastic coupling, which directly couple the order parameters of different origins: one is the ferroelectric phase and another the antiferromagnetic phase.[29]

In marked contrast to the ambient pressure data, the splitting of Mn-O3 and Mn-O4 bonds is less pronounced below T_N at high pressure of 5 GPa: the difference of 0.04 Å at $T=10$ K is smaller than half of the corresponding value at ambient pressure. The reduced distortion in Mn-O3 and Mn-O4 bonds leads to a further symmetric and ideal triangular network of the Mn spins, and so enhanced frustration. The enhanced geometrical frustration effects can then explain the observed appearance of the strong spin fluctuations at low temperatures and a sharp decrease in the ordered magnetic moment. One should note that a direct consequence of the formation of spin-liquid state in $YMnO_3$ at high pressure is the substantially reduced magnetoelastic coupling that facilitates the multiferroic properties, in which linking the physics of multiferroic and geometrical frustrations in a single compound is a unique feature. At ambient pressure, the long-range AFM order onset correlates with an enhancement of the ferroelectric polarization and distortion of Mn-O3 and Mn-O4 bonds, both increased by about 10% well below T_N.[30] A reduced distortion in Mn-O3 and Mn-O4 bonds by about a factor of two at high pressures should lead to subsequent smaller change in the polarization below T_N via a weaker magnetoelastic coupling.

Further insight into high-pressure effects on T_N can be made from the following estimations. Using ambient pressure values of the volume and entropy changes[5,30] at the magnetic ordering temperature, $\Delta V \approx 0.02$ cm^3/mole and $\Delta S \approx 1.25$ J/(mol K), the pressure coefficient of Néel temperature for a moderate pressure range can be estimated from the Clausius-Clapeyron equation as $dT_N/dP=\Delta V/\Delta S=1.6$ K/GPa, quite comparable to the experimentally determined value of 1.2 K/GPa. Some difference between the experimental and calculated values of dT_N/dP can be related to the aforementioned geometrical frustration effects. Alternative estimate comes from an empirical Bloch's rule $d \ln T_N/d \ln V \approx (10/3)$, developed to describe general trends in behavior of T_N of antiferromagnets with localized electrons due to volume change.[31] Using a bulk modulus value $B=120$ GPa for $YMnO_3$ (Ref. 16), we get the value of $dT_N/dP=2.1$ K/GPa, close to the estimate from the Clausius-Clapeyron equation. All this means that the pressure-induced T_N increase can be interpreted as a natural consequence of the enhanced superexchange magnetic interactions for the long-range ordered AFM phase, which is not yet fully suppressed at the experimental pressure range.

IV. CONCLUSIONS

In conclusion, our results show that $YMnO_3$ at high pressure evolves toward short-range ordered spin-liquid ground state coexisting with a suppressed triangular AFM state. A distinctively different temperature dependence of the new spin-liquid phase observed at high pressures from those of the short-range spin correlation at ambient pressure is a clear experimental evidence of their rather different nature. The formation of the spin-liquid phase in $YMnO_3$ occurs through the symmetrization of in-plane Mn-O bond distances at high pressures and implies a substantial reduction in the magnetoelastic coupling, a weaker multiferroic feature.

ACKNOWLEDGMENTS

We dedicate this paper to the memory of Igor Goncharenko, who passed away in a recent tragic accident while preparing the manuscript. Works were supported by the Korea Research Foundation (Grant No. KRF-2005–015-C00153), Center for Strongly Correlated Materials Research, 21st Century Frontier R&D Program for Hydrogen Energy, the Russian Foundation for Basic Research (Grant No. 08–02–90018-Bel-a), and BRFFR-JINR (Grant No. H08D-002).

[1] P. Curie, J. Phys. **3**, 393 (1894).

[2] For a recent review, see M. Fiebig, J. Phys. D **38**, R123 (2005).

[3] T. Kimura, T. Goto, H. Shintani, K. Ishizaka, T. Arima, and Y. Tokura, Nature (London) **426**, 55 (2003); N. Hur, S. Park, P. A. Sharma, J. S. Ahn, S. Guha, and S.-W. Cheong, *ibid.* **429**, 392 (2004); A. Pimenov, A. A. Mukhin, V. Yu Ivanov, V. D. Travkin, A. M. Balbashov, and A. Loidl, Nat. Phys. **2**, 97 (2006).

[4] H. L. Yakel, W. C. Koehler, E. F. Bertaut, and E. F. Forrat, Acta Crystallogr. **16**, 957 (1963).

[5] A. Munoz, J. A. Alonso, M. J. Martinez-Lope, M. T. Casais, J. L.

Martinez, and M. T. Fernandez-Diaz, Phys. Rev. B **62**, 9498 (2000).
[6] T. Katsufuji, M. Masaki, A. Machida, M. Moritomo, K. Kato, E. Nishibori, M. Takata, M. Sakata, K. Ohoyama, K. Kitazawa, and H. Takagi, Phys. Rev. B **66**, 134434 (2002).
[7] P. J. Brown and T. Chatterji, J. Phys.: Condens. Matter **16**, 10085 (2006).
[8] I. Gélard, C. Dubourdieu, S. Pailhès, S. Petit, and Ch. Simon, Appl. Phys. Lett. **92**, 232506 (2008).
[9] P. Schiffer and A. P. Ramirez, Comments Condens. Matter Phys. **10**, 21 (1996).
[10] J. E. Greedan, J. Mater. Chem. **11**, 37 (2001).
[11] E. F. Bertaut, M. Mercier, and R. Pauthenet, Phys. Lett. **5**, 27 (1963).
[12] T. J. Sato, S.-H. Lee, T. Katsufuji, M. Masaki, S. Park, J. R. D. Copley, and H. Takagi, Phys. Rev. B **68**, 014432 (2003).
[13] J. Park, U. Kong, A. Pirogov, S. I. Choi, J.-G. Park, Y. N. Choi, C. Lee, and W. Jo, Appl. Phys. A: Mater. Sci. Process. **74**, S796 (2002).
[14] J. Park, J.-G. Park, G. S. Jeon, H. Y. Choi, C. Lee, W. Jo, R. Bewley, K. A. McEwen, and T. G. Perring, Phys. Rev. B **68**, 104426 (2003).
[15] F. Demmel and T. Chatterji, Phys. Rev. B **76**, 212402 (2007).
[16] D. P. Kozlenko, S. E. Kichanov, S. Lee, J.-G. Park, V. P. Glazkov, and B. N. Savenko, JETP Lett. **82**, 193 (2005).
[17] M. Janoschek, B. Roessli, L. Keller, S. N. Gvasaliya, K. Conder, and E. Pomjakushina, J. Phys.: Condens. Matter **17**, L425 (2005).
[18] D. P. Kozlenko, S. E. Kichanov, S. Lee, J.-G. Park, and B. N. Savenko, J. Phys.: Condens. Matter **19**, 156228 (2007).
[19] T. Lancaster, S. J. Blundell, D. Andreica, M. Janoschek, B. Roessli, S. N. Gvasaliya, K. Conder, E. Pomjakushina, M. L. Brooks, P. J. Baker, D. Prabhakaran, W. Hayes, and F. L. Pratt, Phys. Rev. Lett. **98**, 197203 (2007).
[20] I. N. Goncharenko, I. Mirebeau, P. Molina, and P. Boni, Physica B (Amsterdam) **234-236**, 1047 (1997).
[21] I. N. Goncharenko, V. P. Glazkov, A. V. Irodova, O. A. Lavrova, and V. A. Somenkov, J. Alloys Compd. **179**, 253 (1992); I. N. Goncharenko, High Press. Res. **24**, 193 (2004).
[22] J. Rodríguez-Carvajal, Physica B (Amsterdam) **55**, 192 (1993).
[23] V. B. Zlokazov and V. V. Chernyshev, J. Appl. Crystallogr. **25**, 447 (1992).
[24] E. F. Bertaut and P. Burlet, Solid State Commun. **5**, 279 (1967).
[25] *International Tables for Crystallography*, edited by A. J. C. Wilson (Kluwer Academic, London, 1992), Vol. C.
[26] J. E. Greedan, J. N. Reimers, C. V. Stager, and S. L. Penny, Phys. Rev. B **43**, 5682 (1991).
[27] J. S. Gardner, S. R. Dunsiger, B. D. Gaulin, M. J. P. Gingras, J. E. Greedan, R. F. Kiefl, M. D. Lumsden, W. A. MacFarlane, N. P. Raju, J. E. Sonier, I. Swainson, and Z. Tun, Phys. Rev. Lett. **82**, 1012 (1999).
[28] B. B. Van Aken and T. T. M. Palstra, Phys. Rev. B **69**, 134113 (2004).
[29] Seongsu Lee, A. Pirogov, Misun Kang, Kwang-Hyun Jang, M. Yonemura, T. Kamiyama, S-W. Cheong, F. Gozzo, Namsoo Shin, H. Kimura, Y. Noda, and J.-G. Park, Nature (London) **451**, 805 (2008).
[30] S. Lee, A. Pirogov, J. H. Han, J. G. Park, A. Hoshikawa, and T. Kamiyama, Phys. Rev. B **71**, 180413(R) (2005).
[31] D. Bloch, J. Phys. Chem. Solids **27**, 881 (1966).